

Microstructures and mechanical properties of Mg–8Gd–0.6Zr–xNd ($x = 0, 1, 2$ and 3 mass%) alloys

Qiuming Peng · Yaoming Wu · Daqing Fang ·
Jian Meng · Limin Wang

Received: 9 January 2006 / Accepted: 10 May 2006 / Published online: 10 February 2007
© Springer Science+Business Media, LLC 2007

Abstract Mg–8Gd–0.6Zr–xNd ($x = 0, 1, 2$ and 3 mass%) alloys were prepared by metal mould casting method, and the microstructures, age hardening responses and mechanical properties have been investigated. The microhardness of the as-cast alloys is increased with increasing Nd content. The age hardening behavior and mechanical properties are enhanced significantly by adding Nd element. The peak ageing hardness of the Mg–8Gd–0.6Zr–3Nd alloy is 103, it is about 1.3 times more than that of the Mg–8Gd–0.6Zr alloy. The aged Mg–8Gd–0.6Zr–3Nd alloy exhibits maximum ultimate tensile strength and yield strength, and the values are 271 and 205 MPa at room temperature, 205 MPa and 150 MPa at 250 °C, respectively. Which are about 2 times higher than those of Mg–8Gd–0.6Zr alloy. The improved hardness and strength are mainly attributed to the fine dispersiveness of Mg₅RE and Mg₁₂RE precipitates in the alloy.

Introduction

High performance Mg alloys offer considerable advantages to the automotive and aerospace industries.

Q. Peng · Y. Wu · D. Fang · J. Meng · L. Wang (✉)
Key Laboratory of Rare Earth Chemistry and Physics,
Changchun Institute of Applied Chemistry, Chinese
Academy of Sciences, Changchun 130022, China
e-mail: lmwang@ciac.jl.cn

Q. Peng
Graduate School of the Chinese Academy of Science,
Beijing 100049, China

However, the application of the Mg alloys is very limited due to their low mechanical properties especially at elevated temperature. It is well known that rare earths (RE) have a favorable effect on the mechanical properties of the Mg alloys, such as WE and QE type Mg alloys [1]. More recently, it was confirmed that gadolinium (Gd) and other heavy rare earth elements improve the heat resistance for Mg alloys with metastable and stable phases at relatively elevated temperature [2]. It must be noted that the equilibrium binary phase diagram of Mg–Gd shows eutectic with a solubility of 23.5 mass% Gd at the eutectic temperature 548 °C and 3.8 mass% Gd at 200 °C [3]. Therefore, it is promising to develop a new kind of heat resistance Mg alloy after suitable heat treatment.

However, the Mg–Gd binary alloy containing less than 10 mass% Gd exhibited weak precipitation hardening response during ageing of supersaturated solid solution [4]. Furthermore, high Gd content results in an increase in the densities and the cost, and decreasing elongation of the alloys. Thus, it is necessary to add other elements to substitute the part of Gd for enhancing the mechanical properties. The Nd element is considered because it forms stable Mg-rich binary compounds which might be precipitated during ageing at lower temperature. Some investigations have been done on the Mg–Gd–Nd system alloys. Mg–3Gd–3Nd (mass%) alloy showed remarkable age hardening even at 250 °C, which is related to the β'' phase with a D0₁₉ crystalline structure [5]. The outstanding creep resistance property of sand-cast Mg–2.8Nd–0.3Gd–0.8Zn–0.5Zr (mass%) alloy at 240 °C was associated with small grain size and large activation energy for creep [6]. Meanwhile, it is generally believed that the grain size of the Mg alloys is attributed to the Zr

addition, which is important as a grain refiner because a small amount of the dissolved Zr can provide sufficient solute to activate the undissolved Zr particles in nucleating Mg [7]. Therefore, in the present work, the effect of Nd on the microstructures, age hardening behavior and mechanical properties of the Mg–8Gd–0.6Zr–xNd alloys were investigated.

Experimental procedures

The nominal compositions of investigated alloys are Mg–8Gd–0.6Zr (A), Mg–8Gd–0.6Zr–1Nd (B), Mg–8Gd–0.6Zr–2Nd (C) and Mg–8Gd–0.6Zr–3Nd (D). The alloys were prepared from Mg–20Gd, Mg–20Nd and Mg–30Zr master alloys (mass%) in the graphite crucible under an anti-oxidizing flux. The melting alloys were homogenized at 750 °C for 0.5 h and then cast into a preheated metal mould at approximately 720 °C, the size of ingots is 70 × 40 × 13 mm³. The chemical compositions of obtained ingots were listed in Table 1. The ingots were solution treated at 525 °C for 10 h and subsequently aged at 230 °C.

The microstructures were studied by using optical metallography. The phase compositions and morphology were characterized by X-ray diffraction (XRD) and transmission electron microscope (TEM), respectively. The hardness was carried out by Vickers microhardness tester, and the test load and its application time were 25 g and 15 s. Tensile test was performed using standard tensile testing machining at room temperature (RT) and 250 °C with a strain rate of 1.7×10^{-3} s⁻¹, and the samples took 20 min to balance the temperature before tensile test at 250 °C.

Results and discussion

Microstructures

Figure 1 shows the optical microstructures of the as-cast alloys. It can be seen that the alloys are mainly composed of the coarse continuous network grain boundaries and the matrix, and it is found that the

intercrystalline spacing of the alloys is about 20–50 μm. The XRD patterns of the as-cast alloys are shown in Fig. 2. The results reveal that (A) alloy is mainly composed of α-Mg solid solution and a little amount of Mg₅Gd compound, (B) and (C) alloys consist of α-Mg solid solution and a small amount of Mg₅RE (RE = Gd/Nd), but Mg₄₁RE₅ (RE = Nd/Gd) peaks are observed in (D) alloy with the exception of α-Mg and Mg₅RE phases. The microstructures of the aged alloys at peak ageing hardness are shown in Fig. 3. Comparing to the as-cast state, all the alloys are mainly composed of fine network grain boundaries, and some dispersed precipitates are observed clearly in the matrix. The grain size of the alloys is about 40–100 μm.

Age hardening behavior

Figure 4 shows the age hardening behavior for the alloys. The water quenched hardness (QHV) of the (A) alloy is 71, and it exhibits the weak age hardening response during isothermal ageing. Further increasing Nd content, it can be found that the QHV and PHv are improved clearly. The (D) alloy shows highest QHV and PHv in the investigated alloys, and the QHV is 81 and it takes more than 40 h to reach the PHv of 103. The PHv is almost 1.3 times higher than that of the (A) alloy.

The phase compositions of the (D) alloy by using XRD analysis at different ageing time are shown in Fig. 5. It identifies that the alloy is mainly composed of α-Mg and Mg₃RE (RE = Gd/Nd) phases after aged for 1 h, and α-Mg, Mg₃RE and Mg₁₂RE phases after aged for 40 h, and α-Mg and Mg₅RE phases after aged for 200 h. The TEM image and electron diffraction pattern of the (D) alloy after aged for 40 h is shown in Fig. 6. It can be seen that the quadrat-like precipitates randomly distribute in the α-Mg matrix. According to the XRD result (Fig. 5b) and the electron diffraction pattern, we can confirm the quadrat-like precipitate is stable β-Mg₅RE phase of fcc crystalline structure.

Different compounds were considered to precipitation hardening in Mg alloys containing RE. The increasing hardness of Mg–Nd binary alloy is mainly due to formation of plate shaped GP zones and precipitate on prismatic planes of the Mg matrix [8]. The improved ageing hardness of Mg–15Gd binary alloy is in part associated with the β' metastable phase [4]. However, the strengthening factors are more complicated in ternary Mg–RE alloys. It has been reported that β'-Mg₁₂NdY and β-Mg₁₄Nd₂Y were contributed to precipitation strengthening in WE54 and WE43 alloys [9, 10]. β''-Mg₃RE and β'-Mg₁₅RE₃ phased coexisted and both are of benefit to peak

Table 1 Chemical compositions of the investigated alloys (mass%)

Alloys	Gd	Nd	Zr	Mg
(A)	7.9	–	0.58	Bal.
(B)	7.8	0.7	0.48	Bal.
(C)	7.8	1.8	0.50	Bal.
(D)	7.9	3.1	0.55	Bal.

Fig. 1 The optical microstructures of the as-cast alloys

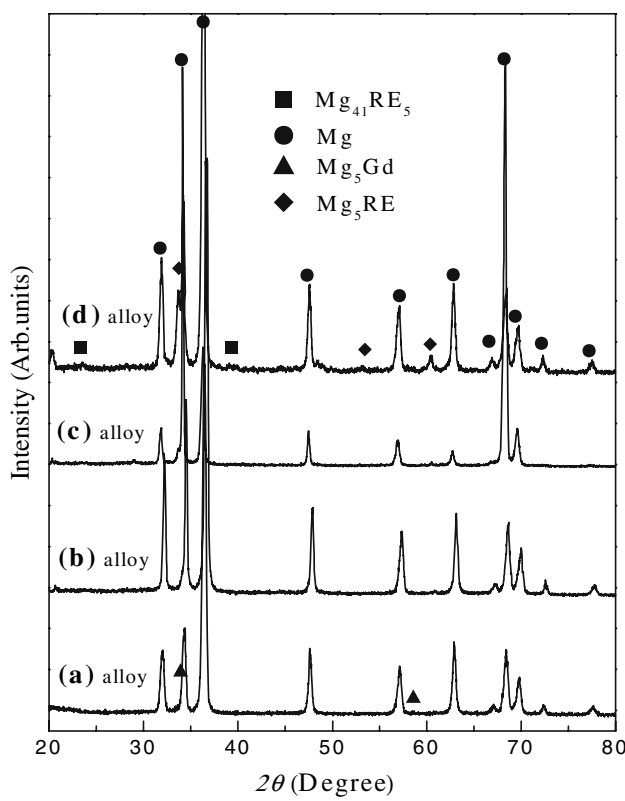
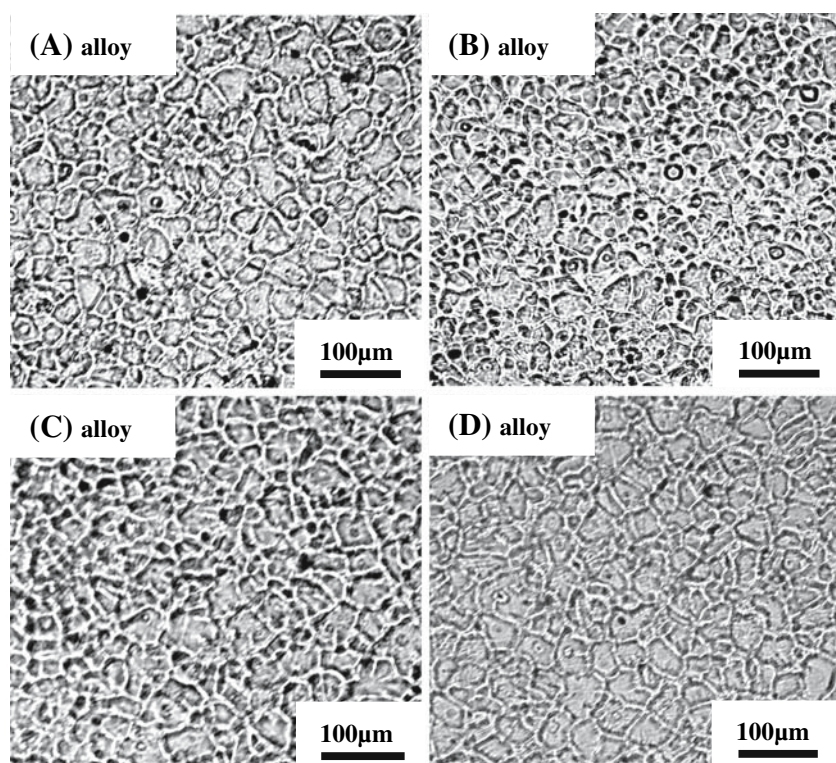


Fig. 2 X-ray diffraction patterns of the as-cast alloys

hardness in Mg–10Gd–3Y–0.45Zr (mass%) alloy [11, 12]. In our investigated alloys, the results of phase compositions indicate that the (D) alloy exhibits

distinctly three-stage decomposition sequence as following:

$$\alpha\text{-Mg(SSS)} - \beta''(\text{Mg}_3\text{RE}) - \beta'(\text{Mg}_{12}\text{RE}) - \beta(\text{Mg}_5\text{RE}).$$

Furthermore, the ageing curves illustrated that the increasing Nd content improved the QHv and PHv for the investigated alloys. The improvement of the QHv is mainly ascribed to solid solution strengthening. The increase of PHv is mainly attributed to precipitation hardening, it is reasonable to confirm that the β' - Mg_{12}RE and β - Mg_5RE precipitates observed at peak aging hardness of the alloys are associated with the enhancement of the PHv. This strengthening mechanism of age hardening behavior for the investigated system alloys is similar to the WE type alloys.

Mechanical properties

Figure 7 shows the typical stress-strain curves of the as-cast alloys at RT. The results demonstrated that the (A) alloy exhibits inferior tensile strength, and the strength was improved notably when added a small amount of Nd. The mechanical properties including ultimate tensile strength (UTS), yield strength (YS) and elongation (ϵ) of the as-cast alloys at RT and 250 °C are listed in Table 2. The UTS and YS are increased monotonically with increasing Nd content. The (D) alloy exhibits highest strength, the UTS and

Fig. 3 The optical microstructures at peak aging hardness of aged alloys

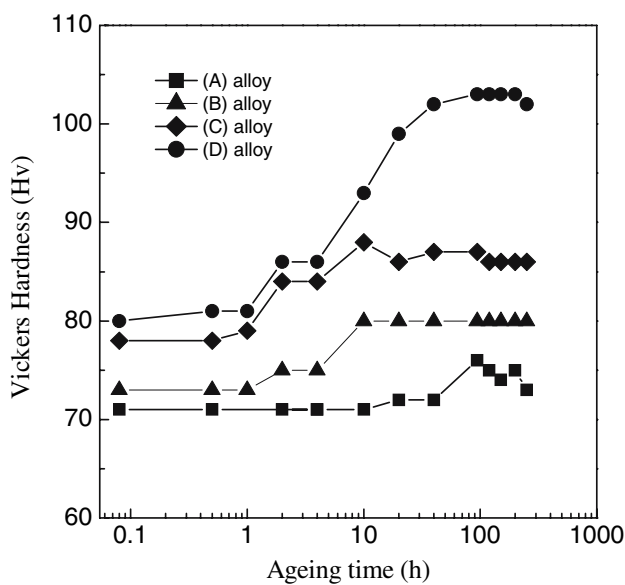
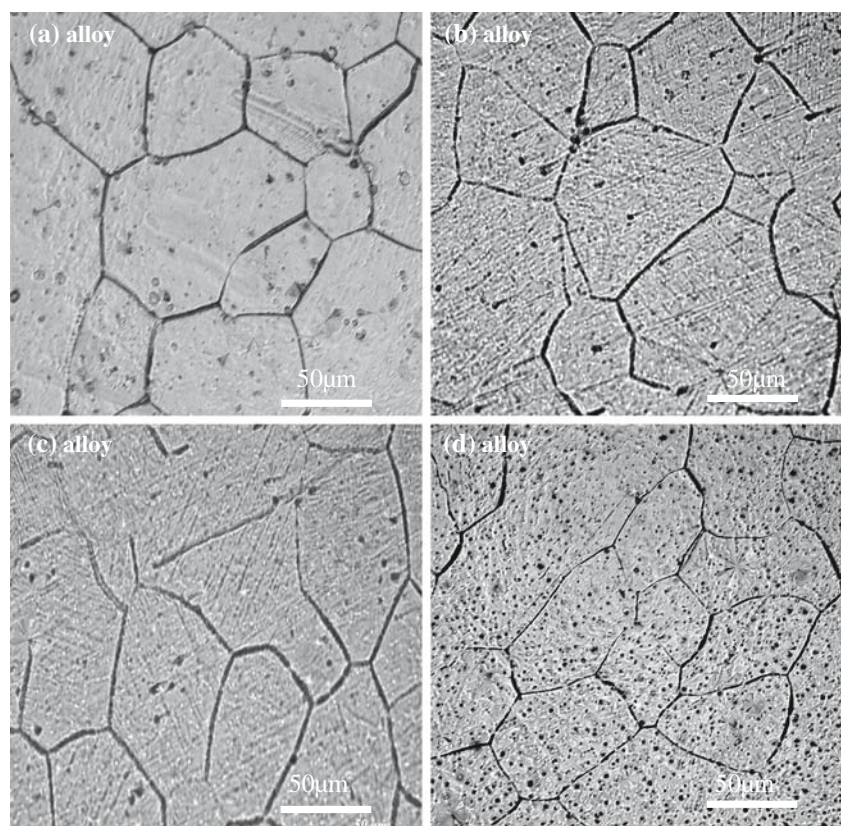


Fig. 4 Age hardness response of the as-cast alloys at 230 °C

YS are 250 MPa and 158 MPa at RT, 210 MPa and 138 MPa at 250 °C respectively. But the largest ε is observed while by adding 1 mass% Nd. The UTS, YS and ε of the aged alloys at PHv are presented in Table 3. Comparing to the as-cast state, the UTS, YS and ε of (A) alloy shows a little change, the (B), (C)

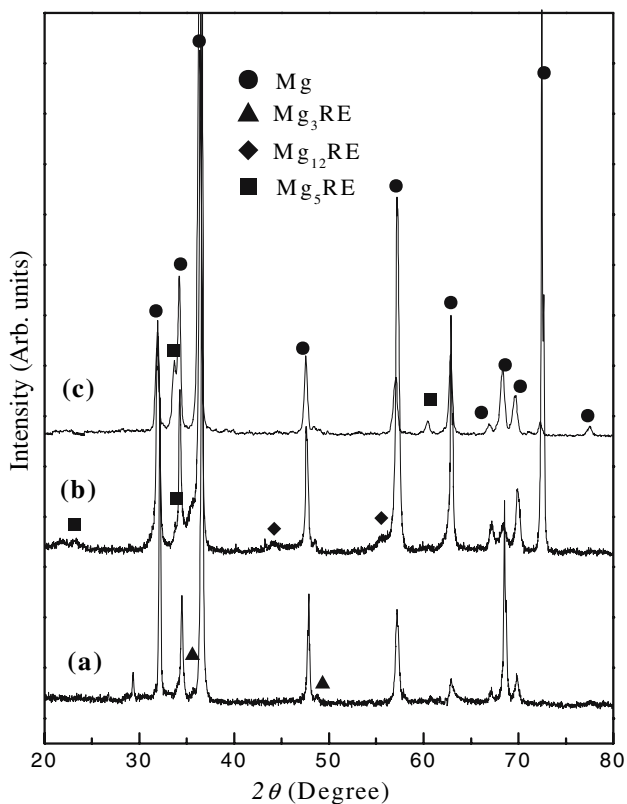


Fig. 5 X-ray diffraction patterns of aged (D) alloys at 230 °C, (a) aged for 1 h, (b) aged for 40 h, (c) aged for 200 h

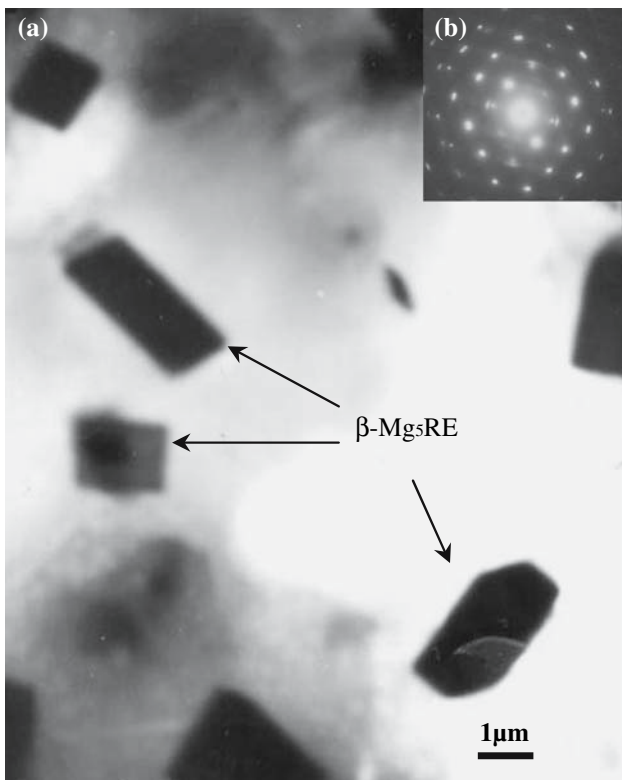


Fig. 6 TEM image and electron diffraction pattern of aged (D) alloy at 230 °C for 40 h, (a) Selected area image, (b) β -Mg₅RE phase parallel to [122] zone axes

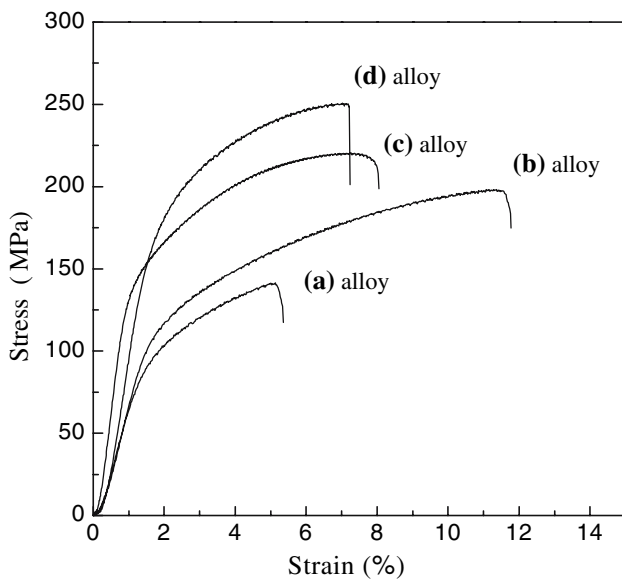


Fig. 7 Relationship between the strain and stress of the as-cast alloys at RT

and (D) alloys improved with increasing Nd content. The (D) alloy exhibits highest UTS and YS, the value are 271 MPa and 205 MPa at RT, 205 MPa and

Table 2 The mechanical properties of as-cast alloys

Alloys	Vickers hardness (Hv)	UTS (MPa)		YS (MPa)		ε (%)	
		RT	250 °C	RT	250 °C	RT	250 °C
(A)	62	141	107	82	74	6.2	11.0
(B)	71	201	189	126	98	11.7	16.6
(C)	76	221	182	137	106	8.2	12.5
(D)	87	250	210	158	138	7.5	11.3

Table 3 The peak ageing hardness and tensile properties of aged alloys

Alloys	PHv	UTS (MPa)		YS (Mpa)		ε (%)	
		RT	250 °C	RT	250 °C	RT	250 °C
(A)	76	155	100	81	74	6.4	9.8
(B)	81	198	183	131	80	8.2	12.4
(C)	87	242	190	172	130	8.0	13.0
(D)	103	271	222	205	150	7.8	12.5

150 MPa at 250 °C, respectively, which are about 2 times higher than that of (A) alloy.

The above results indicate that addition of Nd element to the Mg–8Gd–0.6Zr alloy can improve the mechanical properties, which may be explained from the following factors. Considering the solid solubility of Gd at RT in Mg is low [3], which is reduced by adding other rare earth elements. Adding Nd to the Mg–8Gd–0.6Zr quasi-binary alloy, the solubility limit of Gd will shift largely to lower the concentration with decreasing temperature. In addition, the added Nd element itself has a significant age hardening due to the very little solid solubility in Mg. Consequently, the supersaturated solid solution formed readily and the following aged response was improved correspondingly. Furthermore, the dispersed strengthening phases of the β' (Mg₁₂RE) and β (Mg₅RE) precipitates increase with increasing Nd amount for the investigated Mg–8Gd–0.6Zr–xNd alloys, which are associated with the improvement of mechanical properties. This phenomenon is also observed in Mg–Dy–Nd or Mg–Y–Nd alloys [13, 14], the addition of Nd to the Mg–Dy and Mg–Y binary alloys distinctly decreases the solubility of Dy and Y in the α -Mg matrix and enhances the age behavior.

Conclusions

The addition of Nd could improve the hardness and the age hardening behavior of the Mg–8Gd–0.6Zr alloy significantly. The Mg–8Gd–0.6Zr–3Nd alloy exhibits a maximal peak ageing hardness (103), it is about 1.3

times more than that of the Mg–8Gd–0.6Zr alloy. The mechanical properties increased monotonically with increasing Nd content, the aged Mg–8Gd–0.6Zr–3Nd alloy exhibits maximum ultimate tensile strength and yield strength, the values are 271 MPa and 205 MPa at room temperature, and 205 MPa and 150 MPa at 250 °C, respectively, which are about 2 times higher than that of Mg–8Gd–0.6Zr alloy. The improvement of age hardening and strength is contributed to the β' -Mg₁₂RE and β -Mg₅RE precipitates.

Acknowledgements This work is supported by Chinese Academy of Science for Distinguished Talents Program, and The Science Program of the Promotes Northeast of CAS (KGCX2-SW-216) and Science and Technology Program of Changchun (05GG54). The authors would like to thank Mr. Jianli Wang and Baozhong Liu for benefic discussions.

References

1. Mordike BL, Ebert T (2001) Mater Sci Eng A 302:37
2. Smola B, Stulíková I, von Buch F, Mordike BL (2002) Mater Sci Eng A 324:113
3. Spedding FH, Daane AH (1961) In: The rare earths. John Wiley & Sons, New York and London, p 355
4. Vostrý P, Stulíková I, Smola B, von Buch F, Mordike BL (1999) Phys Stat Sol A 175:491
5. Negishi Y, Nishimura T, Kiryuu M, Kamado S, Kojima Y, Ninomiya R (1995) J Jpn Inst Light Metals 45:57
6. Bell A, Srivastava V, Greenwood GW, Jones H (2004) Z Metallkd 95:369
7. Lee YC, Dahle AK, St John DH (2000) Mater Trans 31:2895
8. Vostrý P, Stulíková I, Smola B, Kiehn J, Riehemann W, Mordike BL (1994) Key Eng Mater 97:29
9. Antion C, Donnadieu P, Perrard F, Deschamps A, Tassin C, Pisch A (2003) Acta Mater 51:5335
10. Nie JF, Muddle BC (2000) Acta Mater 48:1691
11. Anyanwu IA, Kamado S, Kojima Y (2001a) Mater Trans 42:1206
12. Anyanwu IA, Kamado S, Kojima Y (2001b) Mater Trans 42:1212
13. Apps PJ, Karimzadeh H, King JF, Lorimer GW (2003a) Scripta Mater 48:1023
14. Apps PJ, Karimzadeh H, King JF, Lorimer GW (2003b) Scripta Mater 48:475